The Effect of Viscous Dissipation on Forced Convection in a Channel Occupied by a Porous Medium with Counter Flow Arrangement

Nagabhushanam Kotloni [a],
[a] Department of Mathematics, AMCEC-Bangalore,
VTU Research scholar ,R&D Centre, PESIT,
Bangalore-85, India.

V. Leela[b],
[b] Department of S & H ,
PESIT-Bangalore, India.

R. Gangadhara Reddy [c]
[c] Department of Mathematics,
AMCEC-Bangalore, India.

Abstract: **This paper is related to obtain an analytical solution for counter flow forced convection in a parallel plate channel occupied by a layered saturated porous medium under the effect of viscous dissipation. In this problem asymmetrical constant heat flux boundary conditions are considered. Brinkman model is applied for the porous medium. It is found that there is no effect of viscous dissipation in Darcy limits. The effects of viscous dissipation for clear fluid limits are discussed. The effect of viscous dissipation is to increase the Nusselt number both in parallel and counter flow cases**.

Key words: Viscous Dissipation, Counterflow, Forced Convection, Bioheat Transfer, Brinkman Model.

I. INTRODUCTION

Many scientists view life from either the macroscopic (systems) or the microscopic (cellular) level, but in reality one must be aware that life processes exist continuously throughout the spectrum. The measurement and control of temperature in living tissues is of great value in both the assessment of normal physiological function and the treatment of pathological states [1]._With the advancements in biology, health and medicine becoming interdisciplinary, physical and mathematical concepts are being increasingly invoked to model biological processes. Porous medium modeling of bio-fluid and heat flow is an interesting and useful approach to simplify and understand the biological phenomena.

A generic region of biological tissue irrigated by blood flow can readily be perceived to fit our definition of a porous medium comprising a stationary solid (tissue) matrix saturated by fluid (blood) flow, with identifiable interfaces [2]. The heat transport in such biological tissue region can be modeled as convection in porous media with internal heat generation, Zhang [3]. From this perspective, it is apparent that the investigation of heat transfer processes in such a tissue-blood region would require an energy conservation statement similar to the porous medium energy conservation equation.

Effects of heterogeneity in forced convection in a porous medium are studied by Nield and Kuznetsov [4] in a parallel plate channel or a circular duct. The effects of variation of permeability and thermal conductivity, on fully developed forced convection in a parallel plate channel or a circular duct filled with a saturated porous medium, is investigated analytically on the basis of the Darcy and Dupuit-Forchheimer model.

Modeling bioheat transfer with counter flow using porous medium has gained interest in recent years. Flow and heat transfer in biological tissues are analyzed by Khaled and Vafai [5]. They have studied the transport in porous media using mass diffusion and different convective flow models such as Darcy and Brinkman models, along with energy transport in tissues. They have reviewed the possibility of reducing the flow instabilities using porous media. The role of porous media in biomedical engineering related to magnetic resonance imaging (MRI) and drug delivery are reviewed by K Khanafer and Vafai[6]. The role of transport theory in porous media helps in advancing the progress of biomedical applications. The study paves the road for the researchers in the area of MRI and drug delivery to develop comprehensive models based on porous media theory.

Macroscopic governing equations for bioheat transfer phenomena are studied by Nakayama, Kuwahara and Lui [7]. The volume averaging theory of porous media has been applied to obtain a general set of macroscopic governing equations for countercurrent bioheat transfer between terminal arteries and veins in the circulatory system. Capillaries providing a continuous connection between the countercurrent terminal arteries and veins are modeled introducing the perfusion bleed-off rate. A volume averaging theory established in the field of fluid saturated porous media is used, a general bioheat transfer model based on the theory of porous media by Nakayama and Kuwahara [8] to derive a general set of bioheat transfer equations for blood flows and its surrounding biological tissues.

A new simplified bioheat equation for the effect of blood flow is studied by Wienbaum and Jiji [9]. They have derived a new simplified bioheat equation to describe the effect of blood flow on blood tissue heat transfer. In the theoretical and experimental studies, the authors have demonstrated that the isotropic blood perfusion term in existing bioheat equation is negligible because of the microvascular organization.

Viscous dissipation is of interest for many applications. The viscous dissipation effect is an irreversibility that must be accounted for in the first law of thermodynamics formulation of the energy balance statement for any thermodynamic system that involves flow. It is understood as a local production of thermal energy through the mechanism of viscous stresses. Naturally, it is also present in convection flows through porous media [2]. Forced convection with viscous dissipation in a parallel plate channel filled by a saturated porous medium is investigated numerically by Hooman and Gurgenci [10] and have concluded that with isothermal walls, the Brinkman number significantly influences the developing Nusselt number but not the asymptotic one at constant wall heat flux. Both the developing and the asymptotic Nusselt numbers are affected by the value of the Brinkman number. Forced convection with viscous dissipation using a two-equation model in a channel filled by a porous medium is studied by Chen and Tso [11]. They have considered two-equation model that includes viscous dissipation in the fluid phase is solved analytically and exact solutions for the temperature fields are obtained.

Nield [12] presented an analysis to understand when viscous dissipation would be significant in porous medium flows, by comparing the orders of magnitude of the dissipation terms with the thermal diffusion terms in the energy equation. In forced convection, there is a velocity scale present in the form of free stream velocity or the channel cross section averaged velocity. The effects of viscous dissipation on thermal entrance heat transfer in a parallel plate channel filled with a saturated porous medium have been investigated analytically by Hooman, Mofid and Gorji-Bandpy[13], on the basis of a Darcy model. The local and the bulk temperature distribution along with the Nusselt number in the thermal entrance region are discussed and have observed that neglecting the effects of viscous dissipation would lead to the well-known case of internal flows, with the Nusselt number equal to 4.93. An analytical study related to fully-developed laminar forced convection in a parallel-plate channel occupied by a nanofluid or by a porous medium saturated by a nanofluid, subject to uniform-flux boundary conditions is studied by Nield and Kuznetsov[14]. They have adopted a model incorporating the effects of Brownian motion and thermophoresis. They have determined that the combined effect of these two agencies is to reduce the Nusselt number.

Nield and Kuznetsov [15] have obtained an analytical solution for forced convection in a parallel plate channel, with asymmetric constant heat-flux boundaries, occupied by a layered saturated porous medium modeled by the Brinkman equation. Results for the Nusselt number are presented for the cases of the Darcy limit and the clear fluid limit. They found that the effect of counterflow is to reduce the value of the Nusselt number, to values that can be negative and to zero in symmetric velocity profiles.

Nield and Kuznetsov [16] presented an analytic investigation of forced convection in parallel-plate channel partly occupied by a bidisperse porous medium and partly by a fluid, where the distribution being asymmetrical. The dependence of the Nusselt number on conductivity ratio, velocity ratio, volume fraction, internal heat exchange parameter, and the position of the porous-fluid interface have been investigated. It has been shown that for asymmetric heating, a singular behaviour of the Nusselt number is satisfactory.

In this paper we have considered the bioheat transfer problem to investigate the effect of viscous dissipation on forced convection in a channel occupied by a porous medium. It is evident that the main feature that distinguishes bioheat transfer from other forms of heat transfer is the counterflow which is considered in this paper along with viscous dissipation effect.

NOMENCLATURE

C_p	Specific heat at constant pressure of the fluid
G	Applied pressure gradient
H	Channel width
k	Effective thermal conductivity
K	Permeability
M	Pressure-gradient modified viscosity ratio, $\dfrac{\mu_{eff}}{\gamma\mu}$
N	Pressure-gradient modified reciprocal Darcy number, $N = \dfrac{H^2}{\gamma K}$
Nu	Nusselt number defined in Eq. (12)
s	$\dfrac{M_2}{M_1}$ or $\dfrac{N_2}{N_1}$
D	$\dfrac{\mu\rho CpU^2}{\bar{K}\,\bar{u}^2(T_m - T_{w\mu})}$
P, Q, R, S	Quantities defined in Eq. (22)
q''_μ	Mean wall heat flux, $\dfrac{1}{2}(q''_{w1} + q''_{w2})$
q''_w	Wall heat flux
T^*	Temperature
T_m	Bulk mean temperature $T_m = \dfrac{1}{HU}\int_0^H u^* T^* dy^*$
T_w	Wall temperature
$T_{w\mu}$	Mean of the two wall temperatures, $\dfrac{1}{2}(T_{w1} + T_{w2})$
$\hat{T}$	Dimensionless temperature, $\dfrac{T^* - T_{w\mu}}{T_m - T_{w\mu}}$,
u	Dimensionless filtration velocity, $u = \dfrac{\mu u^*}{G_{ref} H^2}$
u^*	Filtration velocity
$\hat{u}$	Rescaled dimensionless velocity, $\dfrac{u^*}{U}$

International Journal of Engineering Research & Technology (IJERT)
ISSN: 2278-0181
Vol. 5 Issue 06, June-2016

$$\hat{u}_1 = \frac{u_1}{\bar{u}},\ \hat{u}_2 = \frac{u_2}{\bar{u}},$$

$\bar{u}$ Dimensionless mean velocity

$$\bar{u} = \int_0^{\xi} u_1 dy + \int_{\xi}^{1} u_2 dy$$

U Mean velocity $U = \frac{1}{H}\int_0^H u^* dy^*$

x Dimensionless longitudinal coordinate, x^*/H

x^* Longitudinal coordinate

y Dimensionless longitudinal coordinate, y^*/H

y^* Longitudinal coordinate

Greek symbols

β Parameter defined in Eq. (15)

γ Parameter controlling applied pressure gradient, $G = \pm\gamma G_{ref}$

λ Parameter $\lambda = \sqrt{\frac{N}{M}}$,

μ Fluid viscosity

μ_{eff} Effective viscosity

ξ Position of the interface between the two layers

ρ Fluid density

ϕ Viscous dissipation

Subscripts

1 Parameters of the first layer, $0 < y^* < \xi H$

2 Parameters of the second layer, $\xi H < y^* < H$

II. MATHEMATICAL FORMULATION

The physical configuration is shown in fig1. It consists of a parallel plate channel occupied by a layered saturated porous medium with counter flow. For the steady state fully developed condition we have unidirectional flow in the x-direction between impermeable boundaries at $y^*=0$ and $y^*=H$. we assume that the permeability K and the effective thermal conductivity k are functions of y^* only. Then the Brinkman momentum equation is

$$\mu_{eff}\frac{d^2u^*}{dy^{*2}} - \frac{\mu}{K}u^* + G = 0 \tag{1}$$

Where μ_{eff} is an effective viscosity, μ is the fluid viscosity, K is the permeability, and G is the applied pressure gradient. We suppose (presume) that μ_{eff}, K and G take different values in the two layers. We assume that

$K = K_1$, $\mu_{eff} = \mu_{eff1}$, $G = \gamma_1 G_{ref}$

for $0 < y < \xi H$, (2a)

$K = K_2$, $\mu_{eff} = \mu_{eff2}$, $G = -\gamma_2 G_{ref}$

for $\xi H < y < H$, (2b)

We define dimensionless variables

$$x = \frac{x^*}{H},\quad y = \frac{y^*}{H},\quad u = \frac{\mu u^*}{G_{ref}H^2} \tag{3}$$

The dimensionless forms of Eq.(1) are

$$M_1\frac{d^2u_1}{dy^2} - N_1u_1 + 1 = 0 \tag{4a}$$

$$M_2\frac{d^2u_2}{dy^2} - N_2u_2 - 1 = 0 \tag{4b}$$

Where the pressure gradient modified viscosity ratios M_1, M_2 and the pressure gradient modified reciprocal Darcy numbers N_1, N_2 are defined by

$$M_1 = \frac{\mu_{eff1}}{\gamma_1\mu},\quad M_2 = \frac{\mu_{eff2}}{\gamma_2\mu},\quad N_1 = \frac{H^2}{\gamma_1K_1},\quad N_2 = \frac{H^2}{\gamma_2K_2} \tag{5}$$

Eq. (4) is solved subject to the boundary conditions

$u_1 = 0$ at $y = 0$, $y = \xi$, and

$u_2 = 0$ at $y = \xi$, $y = 1$ (6)

The solution of Eq. (4) subject to boundary conditions (6) is

$$u_1 = \frac{1 + e^{\lambda_1\xi} - e^{\lambda_1 y} - e^{\lambda_1(\xi - y)}}{N_1(1 + e^{\lambda_1\xi})} \tag{7a}$$

$$u_2 = -\frac{1 + e^{-\lambda_2(1-\xi)} - e^{-\lambda_2(1-y)} - e^{-\lambda_2(y-\xi)}}{N_2(1 + e^{-\lambda_2(1-\xi)})} \tag{7b}$$

Where $\lambda_1 = \sqrt{\frac{N_1}{M_1}}$, $\lambda_2 = \sqrt{\frac{N_2}{M_2}}$

When $\lambda_1 \to \infty$, $\lambda_2 \to \infty$ (Darcy limit) and $\lambda_1 \to 0$, $\lambda_2 \to 0$ (clear fluid limit), the results co-inside with Nield & Kuznetsov.

The Dimensionless mean velocity

$$\bar{u} = \int_0^{\xi} u_1 dy + \int_{\xi}^{1} u_2 dy \tag{8}$$

$$\bar{u} = \frac{1}{N_1}\left\{\xi - \frac{2}{\lambda_1}\frac{(e^{\lambda_1\xi} - 1)}{(e^{\lambda_2\xi} + 1)}\right\} - \frac{1}{N_2}\left\{1 - \xi - \frac{2}{\lambda_2}\frac{(e^{\lambda_2(1-\xi)} - 1)}{(e^{\lambda_2(1-\xi)} + 1)}\right\}$$

For the Darcy limit ($\lambda_1 \to \infty$, $\lambda_2 \to \infty$)

$$\bar{u} = \left(\frac{\xi}{N_1} - \frac{(1-\xi)}{N_2} \right) \tag{9}$$

For the clear fluid limit ($\lambda_1 \to 0$, $\lambda_2 \to 0$)

$$\bar{u} = \frac{1}{6}\left(\frac{\xi^3}{M_1} - \frac{(1-\xi)^3}{M_2} \right) \tag{10}$$

Now suppose that the thermal conductivity is given by

$$\begin{aligned} k &= k_1 \ \text{for} \ 0 < |y^*| < \xi H \\ k &= k_2 \ \text{for} \ \xi H < |y^*| < H \end{aligned} \tag{11}$$

So that the mean value is given by

$$\bar{k} = \xi k_1 + (1-\xi) k_2$$

we write

$$\tilde{k}_i = \frac{k_i}{\bar{k}} \quad \text{for } i = 1,2$$

We define the Nusselt number Nu based on the channel width as

$$Nu = \frac{H q''_\mu}{\bar{k}(T_{w\mu} - T_m)} \tag{12}$$

Where q''_μ is the mean wall heat flux, shown in fig. (1) and

$$q''_\mu = \frac{1}{2}(q''_{w1} + q''_{w2})$$

The steady state thermal energy equation is

$$u^* \frac{\partial T^*}{\partial x^*} = \frac{k}{\rho c_p} \frac{\partial^2 T^*}{\partial y^{*2}} + \phi \tag{13}$$

Where $\phi = \mu \left(\frac{\partial u^*}{\partial y^*} \right)^2$

The first law of thermodynamics leads to

$$\frac{\partial T^*}{\partial x^*} = \frac{dT_m}{dx^*} = \frac{2q''_\mu}{\rho c_p H U} = \text{constant}$$

In this case the dimensionless form of the thermal energy equation may be written as

$$\frac{d^2\hat{T}_1}{dy^2} = -\frac{2Nu\hat{u}_1}{\tilde{k}_1} - \frac{\mu U^2 \rho c_p}{\bar{u}^2 \bar{k}\tilde{k}_1 (T_m - T_{w\mu})} \left(\frac{du_1}{dy} \right)^2 \quad 0 < y < \xi \tag{14a}$$

$$\frac{d^2\hat{T}_2}{dy^2} = -\frac{2Nu\hat{u}_2}{\tilde{k}_2} - \frac{\mu U^2 \rho c_p}{\bar{u}^2 \bar{k}\tilde{k}_2 (T_m - T_{w\mu})} \left(\frac{du_2}{dy} \right)^2 \quad \xi < y < 1 \tag{14b}$$

These equations are now solved subject to the boundary conditions

$\hat{T}_1(0) = \beta,\ \hat{T}_2(1) = -\beta,\ \ \hat{T}_1(\xi) = \hat{T}_2(\xi),\ \ \tilde{k}_1 \frac{d\hat{T}_1}{dy}(\xi) = \tilde{k}_2 \frac{d\hat{T}_2}{dy}(\xi)$ Where

$$\beta = \frac{T_{w1} - T_{w2}}{2(T_m - T_{w\mu})} \tag{15}$$

The solution is of the form

$$\hat{T}_1 = \frac{Nu P_1(y) + \beta Q_1(y) + S_1(y)}{R_1} \tag{16a}$$

$$\hat{T}_2 = \frac{Nu P_2(y) + \beta Q_2(y) + S_2(y)}{R_2} \tag{16b}$$

In the Darcy limit the expressions in Eq. (16a, 16b) become

$$P_1(y) = -\tilde{k}_1 N_1 (1-\xi)^2 y + \tilde{k}_1 N_2 (1-\xi) y (2\xi - y) + \tilde{k}_2 N_2 \xi y (\xi - y)$$

$$Q_1(y) = \tilde{k}_1 N_1 N_2 \bar{u} [\tilde{k}_1 (1-\xi) + \tilde{k}_2 (\xi - 2y)]$$

$$R_1 = \tilde{k}_1 N_1 N_2 \bar{u} [\tilde{k}_1 (1-\xi) + \tilde{k}_2 \xi]$$

$$P_2(y) = \tilde{k}_1 N_1 (1-\xi)(1-y)(\xi - y) + \tilde{k}_2 N_1 (2\xi^2 - \xi - 2\xi^2 y + \xi y^2) + \tilde{k}_2 N_2 \xi^2 (1-y)$$

$$Q_2(y) = \tilde{k}_2 N_1 N_2 \bar{u} [\tilde{k}_1 (1 - 2y + \xi) - \tilde{k}_2 \xi]$$

$$R_2 = \tilde{k}_2 N_1 N_2 \bar{u} [\tilde{k}_1 (1-\xi) + \tilde{k}_2 \xi] \quad \text{(17a, 17b, 17c, 17d, 17e, 17f)}$$

In the clear fluid limit the expressions in Eq. (16a, 16b) become

$$P_1(y) = 3\bar{u}\,\bar{k}(T_m - T_{w\mu}) M_1 M_2 [4M_2 y (\xi - y)(y \xi (2\tilde{k}_1 (1-\xi) + \tilde{k}_2 \xi) - y^2 (\tilde{k}_1 (1-\xi) + \tilde{k}_2 \xi)) - 2\tilde{k}_1 M_1 y (1-\xi)^2 (y - y^2 + \xi + \xi y)]$$

$$Q_1(y) = 6\tilde{k}_1 M_1{}^2 M_2{}^2 \bar{u}^2 \bar{k} (T_m - T_{w\mu}) [\tilde{k}_1 (1-\xi) + \tilde{k}_2 \xi - \tilde{k}_1 y]$$

$$S_1(y) = \mu U^2 \rho c_p y\,[M_2^{\,2}(\xi^2(2\tilde{k}_1(1-\xi)+\tilde{k}_2\xi)-(2y^3+3\xi^2 y-4\xi y^2)(\tilde{k}_1(1-\xi)+\tilde{k}_2\xi))-M_1^{\,2}(\tilde{k}_1(4\xi-6\xi^2-3\xi^4)+$$
$$\tilde{k}_2(9\xi^2+\xi^4))]$$

$$R_1 = 6k_1 M_1^{\,2} M_2^{\,2}\bar{u}^2\bar{k}(T_m - T_{w\mu})[\tilde{k}_1(1-\xi)+\tilde{k}_2\xi]$$

$$P_2(y) = 6\bar{u}\bar{k}(T_m - T_{w\mu})M_1 M_2[\tilde{k}_2 M_2 y(\xi-y)\xi^2(1-y)+M_1(y-y^2+\xi+y\xi)(y^2(\tilde{k}_1(1-\xi)+\tilde{k}_2\xi)+y(\tilde{k}_1(\xi^2-1)-2\tilde{k}_2\xi^2)$$
$$-(\tilde{k}_1(1-\xi)+\tilde{k}_2\xi+\tilde{k}_1(\xi^2-1)-2\tilde{k}_2\xi^2)]$$

$$Q_2(y) = -6k_2 M_1^{\,2} M_2^{\,2}\bar{u}^2\bar{k}(T_m - T_{w\mu})[\tilde{k}_1(2-\xi)+\tilde{k}_2\xi+\tilde{k}_1 y]$$

$$S_2(y) = \mu U^2 \rho c_p[\tilde{k}_2 M_2^{\,2}\xi^4(1-y)+M_1^{\,2}(\tilde{k}_1(2+3\xi+\xi^2-5\xi^3-\xi^4)+\tilde{k}_2(\xi+2\xi^2+9\xi^3)-2(\tilde{k}_1(1-\xi)+\tilde{k}_2\xi)$$
$$(y^4+y^2(1+\xi)^2-2y^3(1+\xi))-6(\tilde{k}_1(2\xi^3+\xi^4-2\xi-1)-2\tilde{k}_2(3\xi^2+\xi^4)))]$$

$$R_2 = 6k_2 M_1^{\,2} M_2^{\,2}\bar{u}^2\bar{k}(T_m - T_{w\mu})[\tilde{k}_1(1-\xi)+\tilde{k}_2\xi]$$

(18a, 18b, 18c, 18d, 18e, 18f, 18g, 18h)

Now substituting in the determining compatibility condition

$$\int_0^1 \hat{u}\hat{T}dy = \int_0^{\xi}\hat{u}_1\hat{T}_1 dy + \int_{\xi}^{1}\hat{u}_2\hat{T}_2 dy = 1 \tag{19}$$

yields an expression for the Nusselt number. We used the Mathematica software package to obtain this expression and also to obtain values of Nu for various values of the input parameters.

In the Darcy limit one has

$$\mathrm{Nu} = \frac{6\{-\beta\bar{u}(\tilde{k}_1 N_2 \pm \tilde{k}_2 N_1)\xi(1-\xi)+N_1 N_2\bar{u}^2[\tilde{k}_1(1-\xi)+\tilde{k}_2\xi]\}}{\dfrac{\tilde{k}_1 N_1}{\tilde{k}_2 N_2}(1-\xi)^4+\dfrac{4N_1}{N_2}\xi(1-\xi)^3\mp 6\xi^2(1-\xi)^2+\dfrac{4N_2}{N_1}\xi^3(1-\xi)+\dfrac{N_2\tilde{k}_2}{N_1\tilde{k}_1}\xi^4} \tag{20}$$

Where $\bar{u} = \left(\dfrac{\xi}{N_1} \mp \dfrac{(1-\xi)}{N_2}\right)$

In the clear fluid limit we obtain

$$\mathrm{Nu} = \frac{\begin{gathered}420\{-\beta M_1\bar{u}(\tilde{k}_1 s\xi^3(1-\xi)+\tilde{k}_2\xi(1-\xi)^3)+6M_1^{\,2}s\bar{u}^2((12/7)\tilde{k}_1(1-\xi)+\tilde{k}_2\xi)\}-(\tilde{k}_1\xi^6/M_2)(8D\xi^2 s^2-35D(9+\xi^2))\\ -(\xi/M_1)(-35D\xi^3(\xi-1)^4-43sD(\xi-1)\xi^6+35(1/s)D\xi^3(1+\xi(6\xi-6)))+(2s\xi D(\xi-1)^3/M_2)\\ (-32+\xi(-1314+\xi(-283+\xi(-404+3\xi)))-(2\tilde{k}_1(\xi-1)/(s\tilde{k}_2 M_2))(D(\xi-1)^2(277+\xi(512+\xi(-579+\xi(-188+3\xi)))))\end{gathered}}{17\dfrac{\tilde{k}_1}{\tilde{k}_2 s}(1-\xi)^8+52\xi(1-\xi)^7\dfrac{1}{s}-70\xi^4(1-\xi)^4+52s\xi^7(1-\xi)+17s\dfrac{\tilde{k}_2}{\tilde{k}_1}\xi^8}$$

(21)

Where $\bar{u}$ is given by Eq. (10) and $D = \dfrac{\mu\rho C p U^2}{\bar{k}\bar{u}^2(T_m - T_{w\mu})}$, $\quad s = \dfrac{M_2}{M_1}$

It is interesting to compare the above results with those for the situation where u_2* is reversed in sign, that is the flow in the two layers is in parallel instead of being in anti-parallel. Then from the Equation (8) we get

International Journal of Engineering Research & Technology (IJERT)
ISSN: 2278-0181
Vol. 5 Issue 06, June-2016

$$\bar{u} = \frac{1}{N_1}\left\{\xi - \frac{2}{\lambda_1}\frac{(e^{\lambda_1 \xi}-1)}{(e^{\lambda_2 \xi}+1)}\right\} + \frac{1}{N_2}\left\{(1-\xi) - \frac{2}{\lambda_2}\frac{(e^{\lambda_2 (1-\xi)}-1)}{(e^{\lambda_2 (1-\xi)}+1)}\right\}$$

For the clear fluid limit ($\lambda_1 \to 0$, $\lambda_2 \to 0$)

Therefore $$\bar{u} = \frac{1}{6}\left(\frac{\xi^3}{M_1} + \frac{(1-\xi)^3}{M_2}\right) \qquad (10^*)$$

In place of Eq. (25), in the clear fluid limit the Nu is

$$\mathrm{Nu} = \frac{\begin{array}{l} 420\{-\beta M_1 \bar{u}(\tilde{k}_1 s\,\xi^3(1-\xi) - \tilde{k}_2 \xi(1-\xi)^3) + 6M_1{}^2 s\bar{u}^2((12/7)\tilde{k}_1(1-\xi) + \tilde{k}_2\xi)\} - (\tilde{k}_1\xi^6/M_2) \\ (8D\xi^2 s^2 - 35D(9+\xi^2)) - (\xi/M_1)(-35D\xi^3(\xi-1)^4 - 43sD(\xi-1)\xi^6 + 35(1/s)D\xi^3(1+\xi(6\xi-6))) \\ +(2s\xi D(\xi-1)^3/M2)(-32+\xi(-1314+\xi(-283+\xi(-404+3\xi)) - (2\tilde{k}_1(\xi-1)/(s\tilde{k}_2 M_2))(D(\xi-1)^2 \\ (277+\xi(512+\xi(-579+\xi(-188+3\xi))))) \end{array}}{17\frac{\tilde{k}_1}{\tilde{k}_2 s}(1-\xi)^8 + 52\,\xi\,(1-\xi)^7\,\frac{1}{s} + 70\xi^4(1-\xi)^4 + 52s\xi^7(1-\xi) + 17s\frac{\tilde{k}_2}{\tilde{k}_1}\xi^8}$$

(21*)

Where $\bar{u} = \frac{1}{6}\left(\frac{\xi^3}{M_1} + \frac{(1-\xi)^3}{M_2}\right)$, $\quad D = \frac{\mu\rho CpU^2}{\bar{k}\bar{u}^2(T_m - T_{w\mu})}$, $\quad s = \frac{M_2}{M_1}$.

Eq. (21) and Eq. (21*) can be combined to give

$$\mathrm{Nu} = \frac{\begin{array}{l} 420\{-\beta M_1 \bar{u}(\tilde{k}_1 s\,\xi^3(1-\xi) \pm \tilde{k}_2 \xi(1-\xi)^3) + 6M_1{}^2 s\bar{u}^2((12/7)\tilde{k}_1(1-\xi) + \tilde{k}_2\xi)\} - (\tilde{k}_1\xi^6/M_2) \\ (8D\xi^2 s^2 - 35D(9+\xi^2)) - (\xi/M_1)(-35D\xi^3(\xi-1)^4 - 43sD(\xi-1)\xi^6 + 35(1/s)D\xi^3(1+\xi(6\xi-6))) \\ +(2s\xi\, D(\xi-1)^3/M2)(-32+\xi(-1314+\xi(-283+\xi(-404+3\xi)) - (2\tilde{k}_1(\xi-1)/(s\tilde{k}_2 M_2))(D(\xi-1)^2 \\ (277+\xi(512+\xi(-579+\xi(-188+3\xi))))) \end{array}}{17\frac{\tilde{k}_1}{\tilde{k}_2 s}(1-\xi)^8 + 52\,\xi\,(1-\xi)^7\,\frac{1}{s} \mp 70\xi^4(1-\xi)^4 + 52s\xi^7(1-\xi) + 17s\frac{\tilde{k}_2}{\tilde{k}_1}\xi^8}$$

(21**)

Where $$\bar{u} = \frac{1}{6}\left(\frac{\xi^3}{M_1} \mp \frac{(1-\xi)^3}{M_2}\right) \qquad (10^{**})$$

Here the upper alternative sign refers to the counterflow situation.

III. RESULTS AND DISCUSSION

The aim of the Present study is to know the effect of viscous dissipation in a channel occupied by the porous media when parallel flow is replaced by counterflow. The effect is evident from the observation of various terms in Eq. (21*) and Eq. (10*). The change in sign in the middle term of the denominator of Eq.(21*) from + to – has a minor effect. Other things being equal, the change would decrease the value of Nu by an amount of 15% where as the change would increase the value of Nu without viscous dissipation. The sign of the value of the denominator is always positive for all values of the parameters. The important effect is a result of changes in sign in Eq.(10) and the numerator of Eq.(21). First consider the case of symmetric heating (β=0). Nu cannot become negative because of the term $\bar{u}^2$ in the expression for Nu. When $\bar{u}$ tends to zero i.e., when M_1 and M_2 tends to 1 in Eq.(10) at ξ=0.5 Nu increases indefinitely where as opposite trend is noticed when viscous dissipation effect is not considered in the counterflow arrangement. Second in the case of asymmetric heating $(\beta \neq 0)$ the value for Nu become negative. A negative value of Nu means that the value of $(T_{w\mu} - T_m)$, the difference between the mean wall temperature and the bulk temperature, has a sign opposite to that of q''_{μ} , the mean wall heat flux into the fluid domain. The negative values arise in the case of strong thermal asymmetry and when the product of β and $\bar{u}$ is positive, so that the more strongly heated boundary (and thus the hotter one) is adjacent to the layer in which the weaker flow occurs, other things being equal.

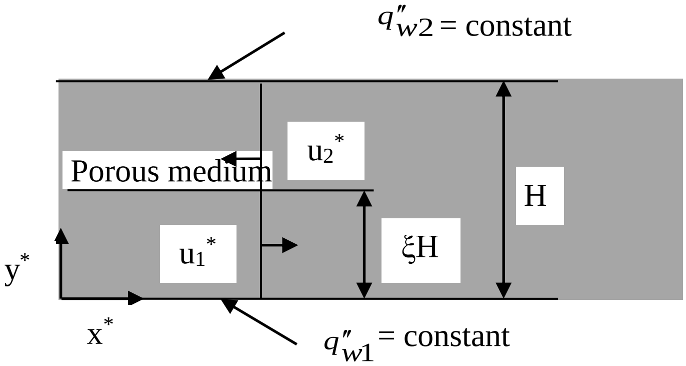

Fig. 1. Definition sketch

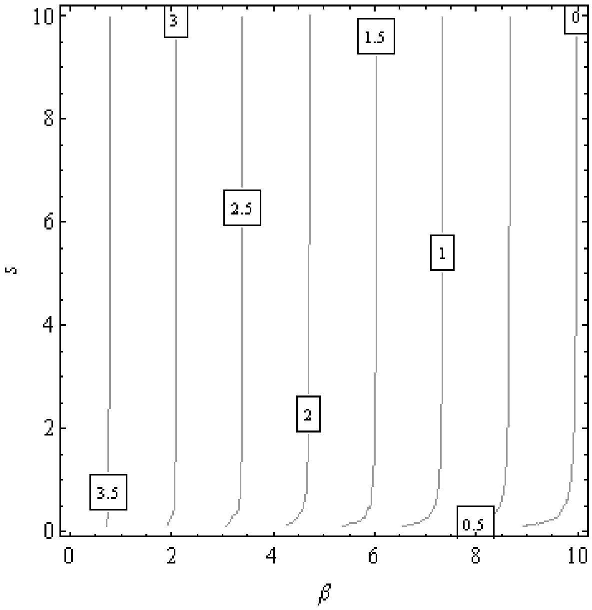

Fig. 2(a) Contour maps of the Nusselt number Nu, as a function of the asymmetric heating parameter β and the flow asymmetry parameter 's', for counter flow when ξ=0.9, D= 0.

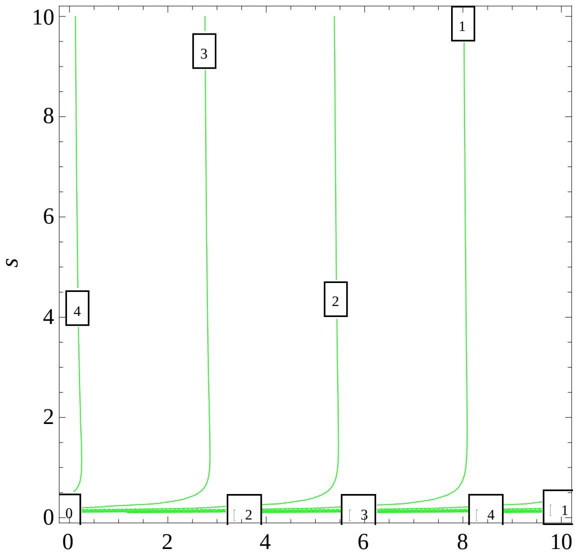

Fig. 2(c) Contour maps of the Nusselt number Nu, as a function of the asymmetric heating parameter β and the flow asymmetry parameter 's', for counter flow when ξ=0.9, D = 0.051220.

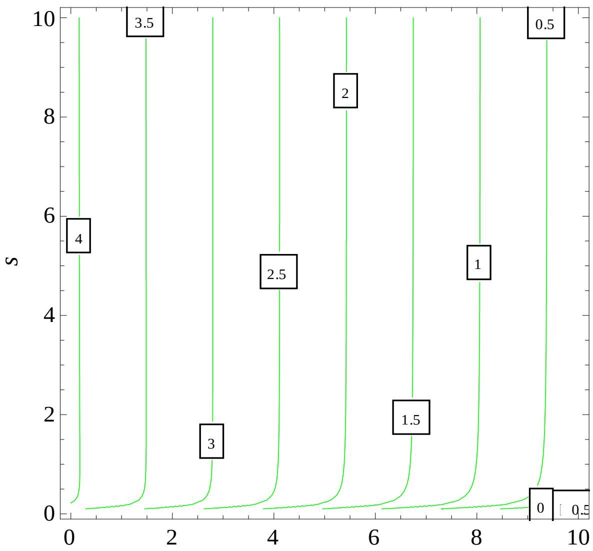

Fig.2(b) Contour maps of the Nusselt number Nu, as a function of the asymmetric heating parameter β and the flow asymmetry parameter 's', for counter flow when ξ=0.9,D = 0.005122.

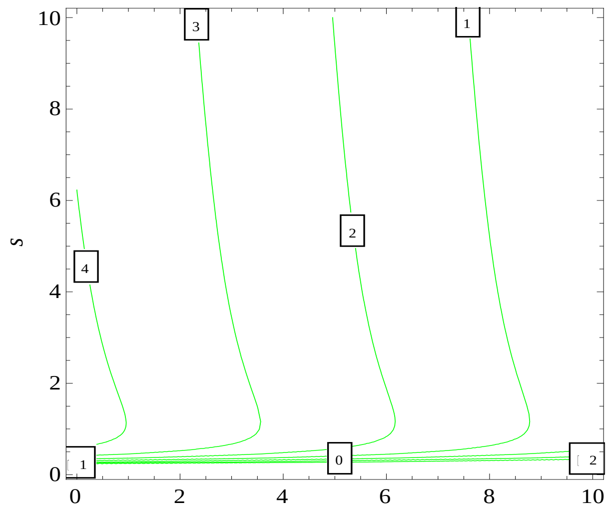

Fig.2(d) Contour maps of the Nusselt number Nu, as a function of the asymmetric heating parameter β and the flow asymmetry parameter 's', for counter flow when ξ=0.9, D = 0.5122.

International Journal of Engineering Research & Technology (IJERT)
ISSN: 2278-0181
Vol. 5 Issue 06, June-2016

For the case of counter flow Fig 2(b) shows the contour maps of Nu as a function of 's' and β when the value of 'D' increases from 0 to 0.005122. The Nu values move towards the right side consequent to this, the contour of Nu value 4 is appearing in Fig 2(b), is not appearing in Fig 2(a). As the value of 'D' increases from 0.005122 to 0.05122, there is not much of a change in the contours of Nusselt number, but it gets curved towards left side in the bottom as seen in Fig 2(c). When the value of 'D' increases from 0.05122 to 0.5122, it can be observed from Fig 2(d) that the contour maps of Nusselt number is more curved towards left side in the bottom.

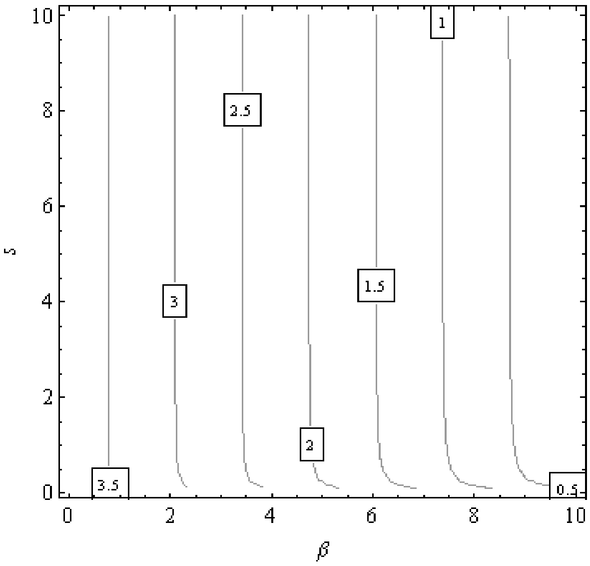

Fig. 3(a) Contour maps of the Nusselt number Nu, as a function of the asymmetric heating parameter β and the flow asymmetry parameter 's', for parallel flow when ξ=0.9, D = 0.

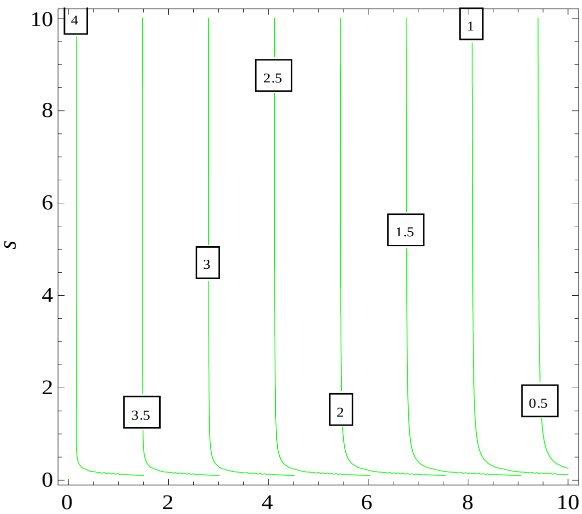

Fig. 3(b) Contour maps of the Nusselt number Nu, as a function of the asymmetric heating parameter β and the flow asymmetry parameter 's', for parallel flow when ξ=0.9, D = 0.0051198.

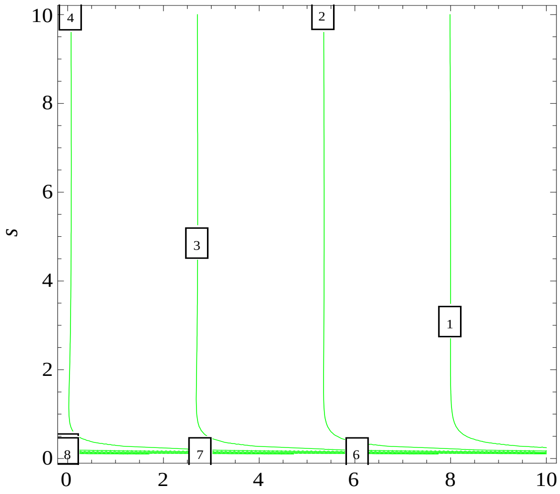

Fig. 3(c) Contour maps of the Nusselt number Nu, as a function of the asymmetric heating parameter β and the flow asymmetry parameter 's', for parallel flow when ξ=0.9, D = 0.051198.

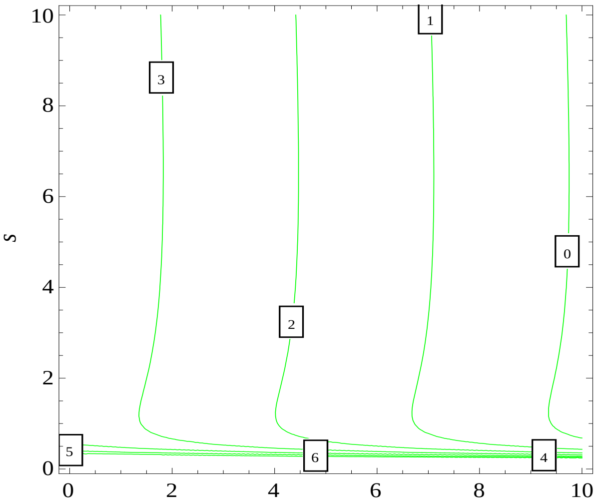

Fig. 3(d) Contour maps of the Nusselt number Nu, as a function of the asymmetric heating parameter β and the flow asymmetry parameter 's', for parallel flow when ξ=0.9, D = 0.51198.

For the case of parallel flow, Fig 3(b) shows the contour maps of Nu as a function of 's' and β when the value of 'D' increases from 0 to 0.0051198. It can be observed from Fig 3(a) and Fib 3(b) that the Nu values move towards the right side. Consequent to this, the contour of Nusselt number value 4 is appearing which can be noted from Fig 3(b) where as in Fig 3(a) it is missing for the range of parameters 's' and β. As the value of 'D' increases from 0.0051198 to 0.051198 there is not much of a change in the contour of Nusselt number, but it gets curved towards right side in the bottom. When the value of 'D' increases from 0.051198 to 0.51198, it can be observed that the contour map of zero Nusselt number appears in Fig 3(d). The other contour of Nusselt number move towards the left side where as contour of Nusselt number 4 does not appear between 2 to 10 of 's' values. Subsequently it can be observed that a contour map of Nu gets more curved and the contour maps of Nusselt number with higher values appear in the bottom.

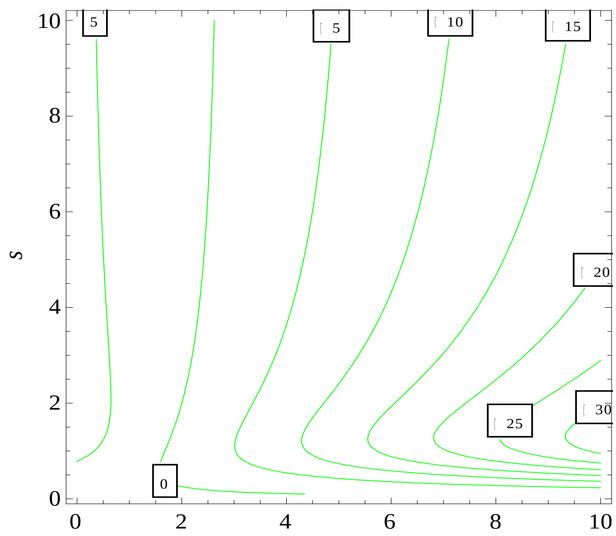

Fig.4(a) Contour maps of the Nusselt number Nu, as a function of the asymmetric heating parameter β and the flow asymmetry parameter 's', for counter flow when ξ=0.5, D = 0.021504.

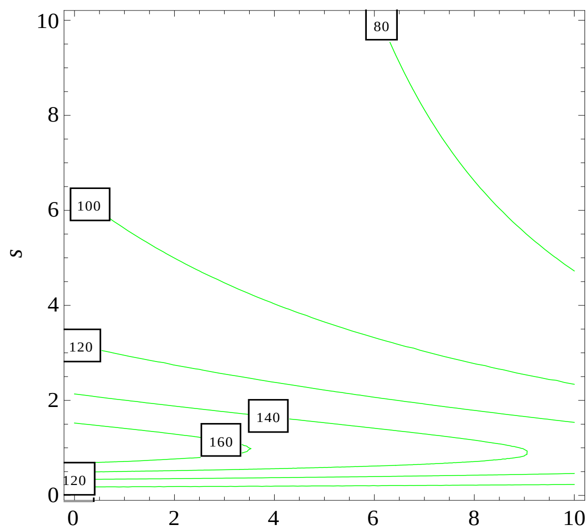

Fig.4(c) Contour maps of the Nusselt number Nu, as a function of the asymmetric heating parameter β and the flow asymmetry parameter 's', for counter flow when ξ=0.5, D = 2.1504.

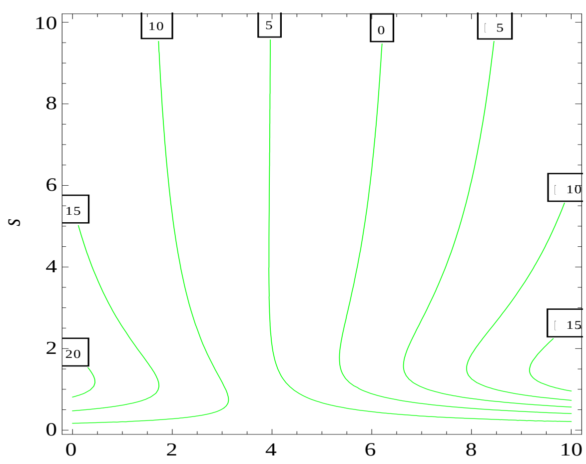

Fig.4(b) Contour maps of the Nusselt number Nu, as a function of the asymmetric heating parameter β and the flow asymmetry parameter 's', for counter flow when ξ=0.5, D = 0.21504.

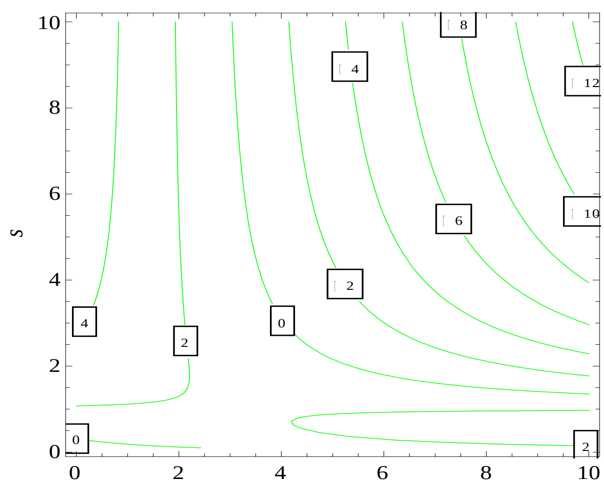

Fig.5(a) Contour maps of the Nusselt number Nu, as a function of the asymmetric heating parameter β and the flow asymmetry parameter 's', for parallel flow when ξ=0.5,D = 0.00032989.

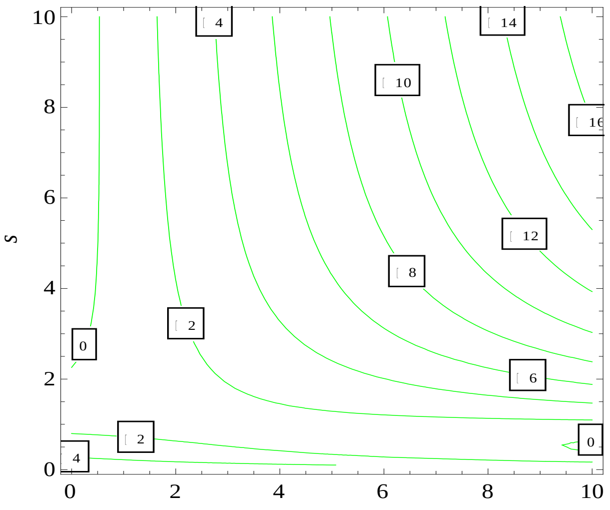

Fig.5(b) Contour maps of the Nusselt number Nu, as a function of the asymmetric heating parameter β and the flow asymmetry parameter ‘s’, for parallel flow when ξ=0.5, D = 0.0032989.

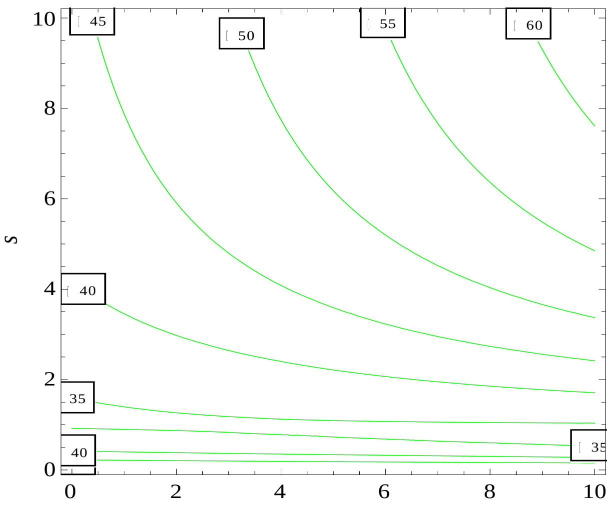

Fig.5(c) Contour maps of the Nusselt number Nu, as a function of the asymmetric heating parameter β and the flow asymmetry parameter ‘s’, for parallel flow when ξ=0.5, D = 0.032989.

Fig 4(a) indicates the contour of Nusselt number for counter flow when ξ=0.5 with D = 0.021504. It can be observed that contour of Nusselt numbers are much smaller like -10, -15, -20, exists on the right side. It can be mentioned here that some of the Nusselt numbers are negative which are consistent with the tables 2(a) and 2(b) of Nield and Kuznetsov [15]. As ‘D’ increases from 0.012504 to 0.21504 the contour of zero Nusselt number moves substantially to the right side which can be observed from the Fig 4(b). The contour of Nusselt number value zero indicates the region where there is no heat transfer and hence bifurcation can be observed. When value of ‘D’ increases from 0.21504 to 2.1504, Nusselt number of contour values have 80, 100, 120 and most of them appear at the bottom portion of the Fig 4(c), indicating higher heat transfer in this region.

For the case of parallel flow when ξ=0.5, Fig 5(b) shows the contour maps of Nu as a function of β and ‘s’. When the value of ‘D’ increase from 0.00032989 to 0.0032989, it can be observed from Fig 5(a) and Fig 5(b), the Nusselt number value zero move towards left side. The contour of much smaller Nusselt number like -50, -55, -60 exists on the right side of the Fig 5(c), indicating less heat transfer in this region.

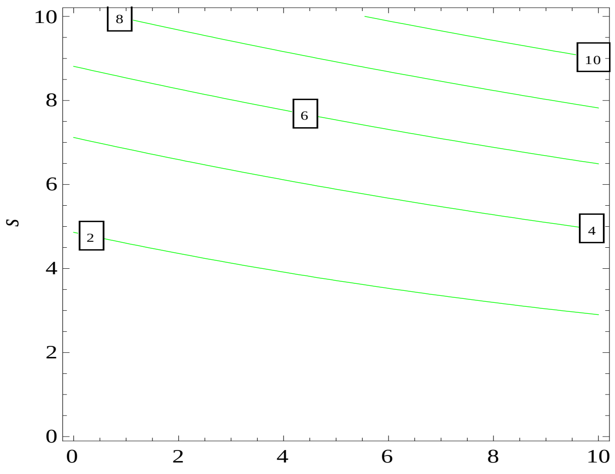

Fig.6(a) Contour maps of the Nusselt number Nu, as a function of the asymmetric heating parameter β and the flow asymmetry parameter ‘s’, for counter flow when ξ=0.1, D = 0.52646.

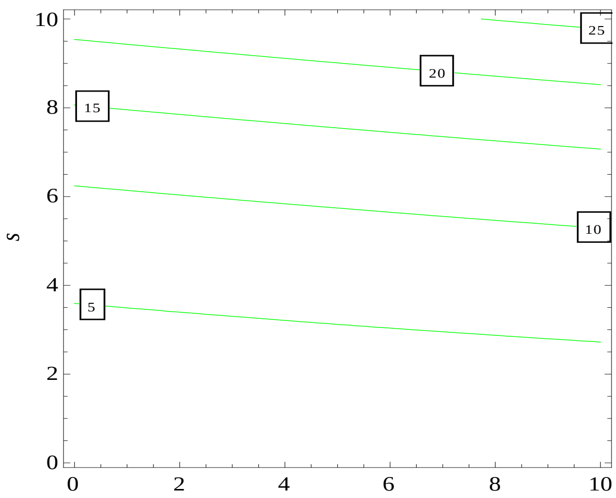

Fig.6(b) Contour maps of the Nusselt number Nu, as a function of the asymmetric heating parameter β and the flow asymmetry parameter ‘s’, for counter flow when ξ=0.1, D = 5.2646 .

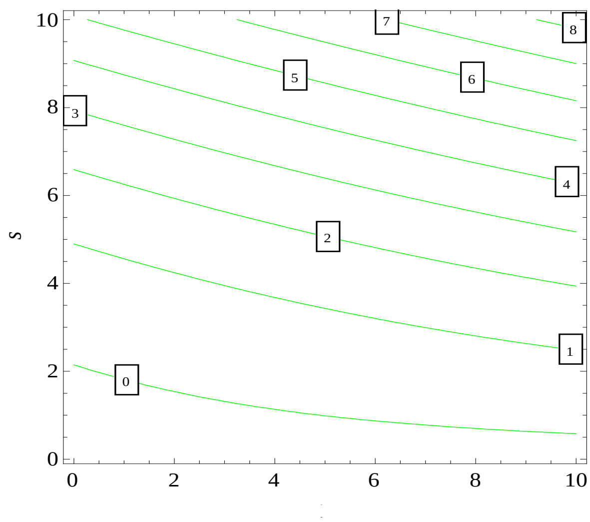

Fig.7(a) Contour maps of the Nusselt number Nu, as a function of the asymmetric heating parameter β and the flow asymmetry parameter 's', for parallel flow when ξ=0.1, D = 0.49835.

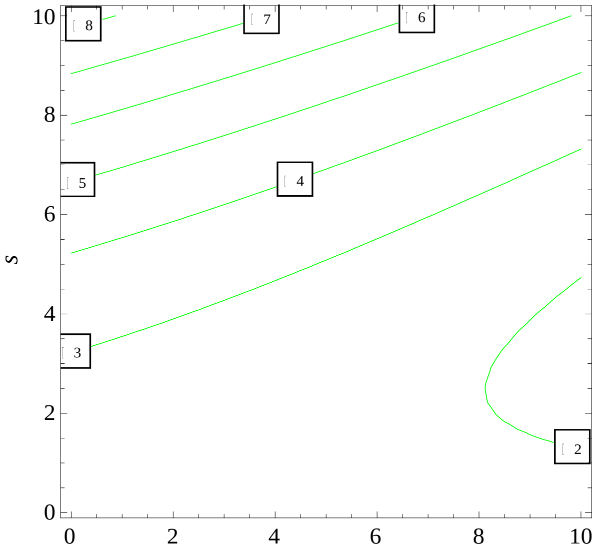

Fig.7(b) Contour maps of the Nusselt number Nu, as a function of the asymmetric heating parameter β and the flow asymmetry parameter 's', for parallel flow when ξ=0.1, D = 4.9835.

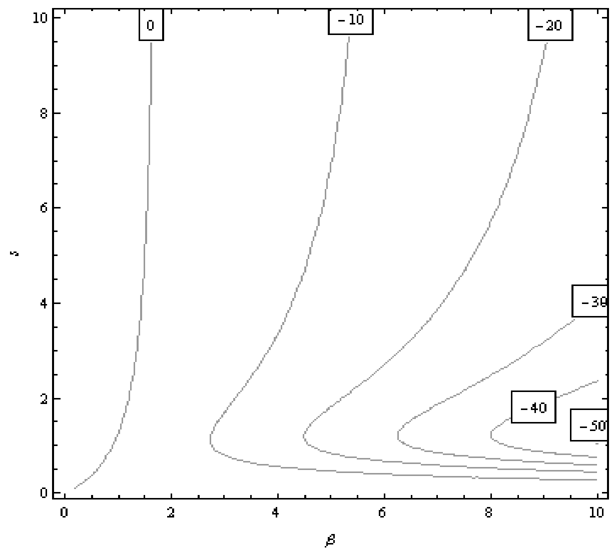

Fig.8(a) Contour maps of the Nusselt number Nu, as a function of the asymmetric heating parameter β and the flow asymmetry parameter 's', for counter flow, for the Darcy limit when ξ=0.5.

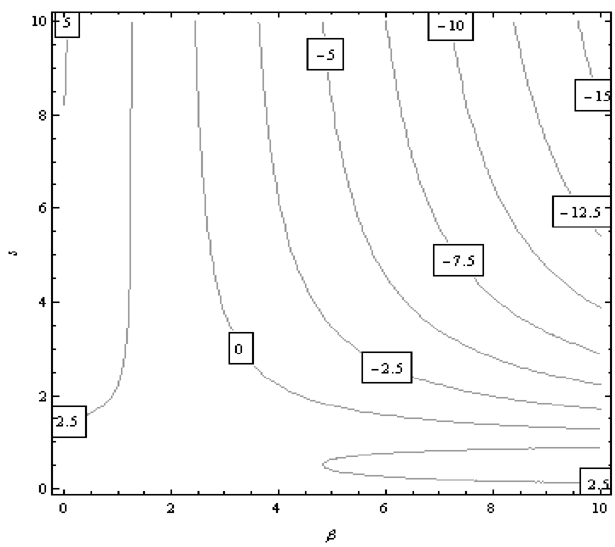

Fig.8(b) Contour maps of the Nusselt number Nu, as a function of the asymmetric heating parameter β and the flow asymmetry parameter 's', for parallel flow, for the Darcy limit when ξ=0.5.

For the case of counter flow when ξ=0.1, D = 0.52646 Nusselt number values appears in upper portions only which is observed from Fig 6(a). When the value of 'D' increases from 0.52646 to 5.2646, the Nusselt number values also increases and appears in the upper portion which can be understood from Fig 6(b).

For the case of parallel flow when ξ=0.1 Fig 7(b) shows the contour map of Nusselt number, when the value of 'D' increases from 0.49835 to 4.9835, the Nusselt number value zero move towards the bottom which can be seen from Fig 7(a) and Fig 7(b).

International Journal of Engineering Research & Technology (IJERT)
ISSN: 2278-0181
Vol. 5 Issue 06, June-2016

TABLE 1(a)

Values of the Nusselt number Nu for counter flow in the Clear fluid limit (Eq. (21)), where $\xi = 0.5$.

	s = 0.1		10	
	Without Viscous dissipation	With Viscous dissipation D = 0.021504	Without Viscous dissipation	With Viscous dissipation D = 0.021504
β = 0	3.62	13.0645	3.62	5.79617
1.0	5.83	15.2754	1.41	3.5853
10	25.73	35.1733	-18.49	-16.3126

TABLE 1(b)

Values of the Nusselt number Nu for parallel flow in the Clear fluid limit (Eq. (21*)), where □= 0.5.

	s = 0.1		1.0		10	
	Without Viscous dissipation	With Viscous dissipation D = 0.0143952	Without Viscous dissipation	With Viscous dissipation D = 0.00435456	Without Viscous dissipation	With Viscous dissipation D = 0.0143952
β = 0	4.42	10.4579	5.38	8.37198	4.42	6.48056
1.0	6.23	12.2652	5.38	8.37198	2.61	4.67329
10	22.49	28.5307	5.38	8.37198	-13.66	-11.5922

TABLE 2(a)

Values of the Nusselt number Nu for counter flow in the Clear fluid limit (Eq. (21)), where □= 0.9.

	s = 0.1		1.0		10	
	Without Viscous dissipation	With Viscous dissipation D = 0.0526461	Without Viscous dissipation	With Viscous dissipation D = 0.0005135	Without Viscous dissipation	With Viscous dissipation D = 0.0005123
β = 0	3.70785	13.404	3.78541	4.06469	3.79317	4.06393
1.0	3.28549	12.9816	3.40167	3.68095	3.41334	3.6841
10	-0.515695	9.18045	-0.0519974	0.227286	-0.00520397	0.265556

TABLE 2(b)

Values of the Nusselt number Nu for parallel flow in the Clear fluid limit (Eq. (21*)), where□= 0.9.

	s = 0.1		1.0		10	
	Without Viscous dissipation	With Viscous dissipation D = 0.0498351	Without Viscous dissipation	With Viscous dissipation D = 0.000511	Without Viscous dissipation	With Viscous dissipation D = 0.000512
β = 0	3.88047	13.0021	3.80267	4.08313	3.7949	4.06578
1.0	3.54494	12.6666	3.42761	3.70807	3.41593	3.68681
10	0.525098	9.64675	0.0520914	0.332551	0.00520491	0.276088

TABLE 3(a)

Values of the Nusselt number Nu for counter flow in the Clear fluid limit (Eq.(21)), where □= 0.1.

	s = 0.1		1.0		10	
	Without Viscous dissipation	With Viscous dissipation D = 0.0005123	Without Viscous dissipation	With Viscous dissipation D = 0.0005135	Without Viscous dissipation	With Viscous dissipation D = 0.0526461
β = 0	3.79317	6.2562	3.78541	6.24477	3.70785	7.65555
1.0	4.17301	6.63604	4.16915	6.62851	4.1302	8.0779
10	7.59155	10.0546	7.62281	10.0822	7.93139	11.8791

TABLE 3(b)

Values of the Nusselt number Nu for parallel flow in the Clear fluid limit (Eq.(21*)), where ξ= 0.1.

	s = 0.1		1.0		10	
	Without Viscous dissipation	With Viscous dissipation D = 0.000512	Without Viscous dissipation	With Viscous dissipation D = 0.00051076	Without Viscous dissipation	With Viscous dissipation D = 0.0498351
β = 0	3.7949	6.25902	3.80267	6.27297	3.88047	7.84183
1.0	4.17387	6.63799	4.17773	6.64803	4.21601	8.17737
10	7.5846	10.0487	7.55325	10.0235	7.23585	11.1972

TABLE 4(a)

Values of the Nusselt number Nu for counter flow in the Darcy limit (Eq. (20)), where □= 0.5.

	s = 0.1	1.0	10.0
β = 0	4.3685	0	4.36854
2	9.70787	0	-0.970787
4	15.0472	0	-6.31011
6	20.3865	0	-11.6494
8	25.7258	0	-16.9888
10	31.0652	0	-22.3281

TABLE 4(b)

Values of the Nusselt number Nu for parallel flow in the Darcy limit (Eq. (20)), where □= 0.5.

	s = 0.1	1.0	10.0
β = 0	5.13982	6	5.13982
2	9.34513	6	0.934513
4	13.5504	6	-3.2708
6	17.7558	6	-7.47611
8	21.9611	6	-11.6814
10	26.1664	6	-15.8867

TABLE 5(a)

Values of the Nusselt number Nu for counter flow in the Darcy limit (Eq. (20)), where □= 0.9.

	s = 0.1	1.0	10.0
β = 0	0.0721414	4.25343	5.04053
2	1.50054	2.33939	3.91915
4	2.92894	0.425343	2.79778
6	4.35734	-1.4887	1.6764
8	5.78574	-3.40275	0.555025
10	7.21414	-5.31679	-0.566352

TABLE 5(b)

Values of the Nusselt number Nu for parallel flow in the Darcy limit (Eq. (20)), where ξ= 0.9.

	s = 0.1	1.0	10.0
β = 0	12.0086	6	5.21585
2	22.2476	6	4.28731
4	32.4866	6	3.35878
6	42.7255	6	2.43024
8	52.9645	6	1.50171
10	63.2034	6	0.57317

TABLE 6(a)

Values of the Nusselt number Nu for counter flow in the Darcy limit (Eq. (20)), where □= 0.1.

	s = 0.1	1.0	10.0
β = 0	5.04053	4.25	0.0721414
2	6.16191	6.16748	-1.35626
4	7.28328	8.08152	-2.78466
6	8.40466	9.99557	-4.21306
8	9.52604	11.9096	-5.64146
10	10.6474	13.8237	-7.06986

TABLE 6(b)

Values of the Nusselt number Nu for parallel flow in the Darcy limit (Eq. (20)), where □= 0.1.

	s = 0.1	1.0	10.0
β = 0	5.21585	6	12.0086
2	6.14438	6	1.7697
4	7.07292	6	-8.46926
6	8.00145	6	-18.7082
8	8.92999	6	-28.9472
10	9.85852	6	-39.1862

As the general solution contains a large number of parameters the discussions are limited to important parameters only. Here we report results only for clear fluid limits. In the case of Darcy limit (i.e. $\lambda_1 \to\infty$, $\lambda_2 \to\infty$) the dissipation term does not exists in Eq.(14a, 14b), which states that there is no effect of viscous dissipation in Darcy limits and we get the results which are similar to that of non viscous dissipation which are plotted in Fig. 8(a), 8(b). In the Darcy limit the effect of increasing β is to decrease Nusselt number. The corresponding Nusselt number values are presented in the tables 4(a) and 4(b) for ξ = 0.5. For ξ = 0.9, 0.1 the results are presented in the tables 5(a), 5(b) and 6(a), 6(b) for both counter flow and parallel flow respectively.

In this study the results are presented for the case of homogeneity of thermal conductivity with viscous dissipation. Therefore we have taken $\tilde{k}_1 = \tilde{k}_2 = 1$. The general effect of the thermal heterogeneity with viscous dissipation can be deduced by inspection from the expression in Eq. (21). In this expression, the denominator is a relatively weak function of $\tilde{k}_2/\tilde{k}_1$ the value is increased by a relatively small percentage as $\tilde{k}_2/\tilde{k}_1$ and moves away from unity in either direction.

At ξ = 0.5, s = 0.1 it is observed from the table 1(a) that for the counterflow in the clear fluid case, Nusselt number value increased by 360.9%, under the influence of viscous dissipation effect for the values of β = 0, 1.0 and 10. As 'β' increases from 0 to 1.0 Nusselt number increased by 1.17% and when 'β' increases from 1.0 to 10 Nusselt number increased by 2.3%. As s tends to 1 Nusselt number becomes very large irrespective of changes in 'β'. When's' increases from 1 to 10 and at s = 10 Nusselt number decreases as β increases.

In the case of thermal homogeneity (with viscous dissipation) and for layers of thickness ξ = 0.9, we obtained the Nusselt number values and are presented in tables 2(a) and 2(b). There is marginal difference between the values of Nu for the different values of 'β' and's' for the counter flow and parallel flow in the clear fluid limits. The effect of increasing β is to decrease Nu for the values of s = 0.1, 1.0 and 10 i.e., $M_2 < M_1$, $M_2 = M_1$ and $M_2 > M_1$.

IV. CONCLUSION

The effect of viscous dissipation for forced convection with counter flow arrangement in a parallel plate channel with asymmetric constant heat flux boundary conditions have been solved analytically. For the case of Darcy flow the viscous dissipation effect is not present. However, for a clear fluid, effect of viscous dissipation exists, and it has been clearly indicated. The effect of viscous dissipation alters the Nusselt number both for parallel and counter flow in clear fluid limits. In the counter flow limits Nusselt number increases as β increases for ξ = 0.1 and 0.5 where as Nusselt number decreases for ξ = 0.9. It is expected that the general trends illustrated by the present model will hold good to specific biological situations.

Conflict of interest:

None declared.

V. REFERENCES

[1] Jonathan W. Valvano, Bioheat Transfer, The University of Texas, Austin, Texas, second edition, 2005.

[2] Arunn Narasimhan, Essentials of Heat and Fluid Flow in Porous Media. Ane. Books Pvt. Ltd., 2013

[3] Zhang, Y, Generalized dual-phase lag bioheat equations based on nonequilibrium heat transfer in living biological tissues. International journal of Heat and Mass Transfer 52, (21-22) 4829-4834, 2009.

[4] D.A.Nield, A.V. Kuznetsov, Effects of heterogeneity in forced convection in a porous medium: parallel plate channel or circular duct. Int. J. Heat and Mass Transfer 43, 4119-4134, 2000.

[5] A. R. A. Khaled, K. Vafai, The role of porous media in modelling flow and heat transfer in biological tissues. Int. J. Heat and Mass Transfer 46, 4989-5003, 2003.

[6] K. Khanafer, K. Vafai, The role of porous media in biomedical engineering as related to magnetic resonance imaging and drug delivery. Heat Mass Transfer 42, 939-953, 2006.

[7] Akira Nakayama, Fujio Kuwahara, W. Lui, Macroscopic Governing Equations for Bioheat Transfer Phenomena. Proceedings of the 2nd International Conference on porous Media and its Application in Science and Engineering ICPM2, 17-21, 2007.

[8] A. Nakayama, F. Kuwahara, A general bioheat transfer model based on the theory of porous media. Int. J. Heat and Mass Transfer 51, 3190-3199, 2008.

International Journal of Engineering Research & Technology (IJERT)
ISSN: 2278-0181
Vol. 5 Issue 06, June-2016

[9] S. Weinbaum, L. M. Jiji, A new simplified Bioheat Equation for the Effect of Blood Flow on Local Average Tissue Temperature. J. BioMech Eng 107(2), 131-139(1985), 2009.

[10] K Hoonam, H Gurgenci, Effects of viscous dissipation and boundary conditions on forced convection in a channel occupied by a saturated porous medium, Transp Porous Med 68, 301-319, 2007.

[11] G.M. Chen, C.P. Tso, Forced convection with viscous dissipation using a two-equation model in a channel filled by a porous medium, International Journal of Heat and Mass Transfer Volume 54, Issues 9–10, April (2011) 1791–1804.

[12] Nield, D. A, Resolution of a paradox involving viscous dissipation and nonlinear drag in a porous medium. Transport in Porous Media 41 (3), 349-357, .2000b.

[13] Hooman Kamel, Gorji-Bandpy Mofid, Effect of Viscous Dissipation on Forced Convection in a Porous Saturated Duct with a Uniform Wall Temperature, Heat Transfer Research, 35, 11 pages, 2005.

[14] D.A. Nield, A.V. Kuznetsov, Forced convection in a parallel-plate channel occupied by a nanofluid or a porous medium saturated by a nanofluid, International Journal of Heat and Mass Transfer, Volume 70, 430–433, 2014.

[15] D.A.Nield, A.V. Kuznetsov, A bioheat transfer model: forced convection in a channel occupied by a porous medium with counterflow. Int. J. Heat and Mass Transfer 51, 5534-5541, 2008.

[16] D.A.Nield, A.V. Kuznetsov, Forced convection in a channel partly occupied by a bidisperse porous medium: asymmetric case. Int. J. Heat and Mass Transfer 53, 5167-5175, 2010.